Simultaneous Tracking and Data Association in an Extended Maneuvering Target Using the IMM Methodology

Daniel Sigalov
Mathematics
Technion - IIT
Haifa, Israel
dansigal@tx.technion.ac.il

Tomer Michaeli
Computer Science and Applied Mathematics
Weizmann Institute of Science
Rehovot, Israel
tomer.michaeli@weizmann.ac.il

Yaakov Oshman
Aerospace Engineering
Technion - IIT
Haifa, Israel
yaakov.oshman@technion.ac.il

***Abstract*—Extended target tracking arises in situations where the resolution of the sensor is high enough to allow multiple returns from the target of interest corresponding to its different parts. Various formulations and solutions may be found in the literature. We concentrate on the data association aspect involved in the tracking problem and propose utilization of a general framework that allows reformulation of many seemingly unrelated problems in a similar way. Consequently, the extended object tracking problem is stated as a single generalized dynamical system with random coefficients and solved using a standard IMM-like algorithm.**

I. INTRODUCTION

Extended, as opposed to point, target tracking arises in situations where the resolution of the sensor is sufficiently high to admit multiple returns from the object of interest corresponding to its various parts. This allows the tracking system to gain valuable information, such as target shape, orientation, and type. Hence, the objective of the system might change from tracking a single point on the target (e.g., its center of mass) to tracking several target features observed by the sensor. However, such modification of the objective introduces new difficulties in comparison to the standard ones arising in point target tracking. These are due to the fact that, despite the high sensor resolution, the returns are noisy and, more importantly, unlabeled. In addition, due to imperfect detection probability, some detections may be missing and clutter returns may be present. In other words, one faces a data association problem which has to be addressed in addition to the actual tracking.

The problem of tracking an extended object has been extensively treated in the literature. Earlier contributions include [1] that was concerned with tracking the centroid of an extended object or a cluster of targets, and [2] that combined a standard multiple model algorithm with an explicit logic to deal with the data association problem. Another method for tracking a cluster of targets, without distinguishing between its members, was proposed in [3]. More recent contributions include [4] and [5], that were concerned with tracking the individual features of an extended target and tackled the problem using particle filtering techniques. The most recent work known to the authors is [6], that deals with the estimation of the shape of an extended object.

In the present work we focus on the data association challenge involved with tracking the individual features of an extended object. Unlike some previous approaches, we do not pursue algorithmic improvement, but, rather, show how the problem may be reformulated and cast into the framework of a single state-space system with random coefficients. Consequently, an approximation to the optimal solution may be obtained using a standard, off-the-shelf IMM algorithm [7], eliminating the need for separate treatment of tracking and data association.

The unified approach to cast seemingly unrelated problems into the same framework has been previously taken by the authors in [8], [9], where we showed how the classical problems of tracking a nonmaneuvering target in clutter and multiple nonmaneuvering targets may be solved using a single IMM-like algorithm after reformulating these problems using a single, generalized dynamical system with random coefficients. Consequently, in [10] we treated the problem of tracking a splitting target in the same context. In the present paper, we follow the same reasoning, and consider tracking an extended maneuvering target. A noticeable difference with regard to our previous work is that, in the present case, we simultaneously address uncertainties in the target dynamics, reflecting random maneuvers, as well as uncertainty in the measurement origin due to the need to associate unlabeled measurements with targets or clutter.

The remainder of the paper is organized as follows. In Section II we give a formal formulation of the considered problem. A brief review of the IMM algorithm is then given in Section III. The IMM-based algorithm is described in Section IV and its performance is demonstrated via a numerical example in Section V. Concluding remarks are given in Section VI.

II. PROBLEM FORMULATION

We consider a set of feature points $i = 1, \ldots, L$ each described by a state vector x_k^i. The object is assumed to be rigid, hence all feature points are assumed to evolve in accordance with the same dynamics. Thus, x_k^i undergoes the following evolution

$$x_{k+1}^i = A_k x_k^i + C_k w_k, \; i = 1, \ldots, L. \tag{1}$$

Here, the process noise $\{w_k\}$ is a zero-mean, unit-covariance white Gaussian sequence, which is assumed to be identical for all the features comprising the object. In addition, A_k

and C_k are random matrices that are assumed to be the same for all features. In other words, in order to satisfy the constraint of a rigidly moving target, we enforce all its components to be driven by the same process noise with the same dynamics. The rigid target model defined above is somewhat simplistic to make the exposition simple and concentrate on the solution methodology. Nevertheless, it does not compromise the solution approach described in Section IV, which may be adopted to more complex formulations as well. For example, it is possible to introduce additional process noise for each feature to represent, e.g., the different velocities of an aircraft wing-tip and its center of gravity.

The pair $\{A, C\}$ is assumed to take discrete values, corresponding to different motion regimes of the target from a set of ℓ models. This set of feasible values, $\{\{A^1, C^1\}, \ldots, \{A^\ell, C^\ell\}\}$, is assumed to be known and may include, e.g., the nearly-constant velocity motion model, or the discrete Wiener process acceleration model [11]. Transitions between different values are captured by a finite state Markov chain with known transition probability matrix (TPM), (p_{ij}), $i, j = 1, \ldots, \ell$, and a known initial distribution. The resulting Markov Jump Linear System (MJLS) is commonly used to model maneuvering targets [11].

We also assume that each feature point is measured through the following measurement model

$$y_k^i = Hx_k^i + Gv_k^i, \quad i = 0, \ldots, L, \tag{2}$$

where $\{v_k^i\}$ are independent zero-mean, unit-covariance white Gaussian sequences. It is assumed that these measurements are unlabeled, such that it is a priori unknown which measurement originates from what feature.

We consider two variants of the feature detection process. First, we assume that each feature is detected with a known probability P_d, independently of other features and measurements at the present or other times. In the second variant, at each time, a feature may go either undetected or obscured. An unobscured feature is detected with a known probability P_d as described above. Alternatively, the target may perform a maneuver during which some of the features are no longer in the field-of-view (FOV) of the sensor. In this variant it is known, for each motion regime, which features are obscured and which are in the sensor's FOV. For example, coordinated turns are usually performed by making appropriate roll maneuvers, thus reducing the visibility of one of the wing-tips from some directions.

In addition to the detections of the actual features, some of the measurements may be false alarms or clutter. These do not carry useful information about the features of interest and are assumed to have uniform spatial distribution defined by G_{cl}, the square-root of its covariance matrix. Clutter measurements are independent of any other statistical quantity that was previously defined.

The goal of this work is to develop an algorithm capable of simultaneously associating and tracking all features of interest.

III. Background on IMM

The IMM method estimates the state of the following system:

$$x_{k+1} = A(\theta_k)x_k + C(\theta_k)w_k \tag{3}$$

$$y_k = H(\theta_k)x_k + G(\theta_k)v_k. \tag{4}$$

Here, $\{w_k\}$ and $\{v_k\}$ are independent, white, zero-mean, unit-covariance Gaussian sequences, x_0 is a Gaussian random vector with known mean and covariance matrix, and $\{\theta_k\}$ is a Markov chain on $\{1, \ldots, r\}$ with some known TPM, (p_{ij}), and initial distribution vector.

At time k, the algorithm recursively estimates x_k using $y_0, \ldots, y_k$ providing an approximation of the MMSE solution. The main idea underlying the IMM algorithm is to maintain a bank of primitive Kalman filters, each matched to a different model in the given model set (different value of θ_k). At step k, the j-th filter produces a local estimate $\hat{x}_k(j)$ with an associated error covariance $P_k(j)$ using its initial estimate $\hat{x}_{k-1}^{\text{init}}(j)$ and the associated covariance $P_{k-1}^{\text{init}}(j)$, which are generated externally, and the current measurement y_k, which gets processed by all KFs in the bank. In addition, each filter produces a current value of its own (model-matched) likelihood function $\Lambda_k(j)$. The key element of the IMM scheme is the interaction block that generates, using all local estimates, covariances, and likelihoods from the previous cycle, individual initial conditions for each of the primitive filters in the bank.

The steps of the algorithm are summarized as follows.

A. Mixing Probabilities

For $i, j = 1, \ldots, r$ compute

$$\begin{aligned}\mu_{k-1}(i \mid j) &\triangleq \mathbb{P}\{\theta_{k-1} = i \mid \theta_k = j, \mathcal{Y}_{k-1}\} \\ &= \frac{1}{c_j} p_{ij}\mu_{k-1}(i),\end{aligned} \tag{5}$$

where

$$\mu_k(i) \triangleq \mathbb{P}\{\theta_k = i \mid \mathcal{Y}_k\}, \quad i = 1, \ldots, r$$

are the posterior mode probabilities that may be computed according to (8) below, c_j is a normalization constant, and $\mathcal{Y}_k \triangleq \{y_0, \ldots, y_k\}$.

B. Mixing Step

For $j = 1, \ldots, r$ compute the initial state estimate for the filter matched to $\theta_k = j$

$$\hat{x}_{k-1}^{\text{init}}(j) = \sum_{i=1}^{r} \hat{x}_{k-1}(i)\mu_{k-1}(i \mid j) \tag{6}$$

and the corresponding covariances.

C. Mode-Matched Filtering

For $j = 1, \dots, r$, using (6) and the corresponding covariance, compute the mode-matched estimate $\hat{x}_k(j)$ and $P_k(j)$ as well as the likelihood $\Lambda_k(j)$, which is approximated as Gaussian

$$\Lambda_k(j) = \mathcal{N}(y_k; \hat{y}_k(j), S_k(j)), \tag{7}$$

where $\hat{y}_k(j)$ and $S_k(j)$ are the predicted measurement and innovation covariance computed by the j-th filter using the initial conditions (6).

D. Mode Probability Update

Compute

$$\mu_k(j) = \frac{1}{c}\Lambda_k(j)\sum_{i=1}^{r} p_{ij}\mu_{k-1}(i), \quad j = 1, \dots, r \tag{8}$$

where c is a normalization factor.

E. Output Computation

At time k, the algorithm's output is obtained as a fused version of the local estimates:

$$\hat{x}_k = \sum_{j=1}^{r} \hat{x}_k(j)\mu_k(j). \tag{9}$$

The associated covariance is computed in a similar manner.

IV. THE PROPOSED SOLUTION

Following the rationale proposed in [9], we show in this section how to solve the problem of tracking an extended maneuvering target using a single, IMM-like, algorithm. To this end, we need to define the Markov mode sequence $\{\theta_k\}$ and specify the matrices $A(\theta_k)$, $C(\theta_k)$, $H(\theta_k)$, and $G(\theta_k)$.

Recall that at each time instant k, there are L features that evolve according to the dynamics defined in (1). In addition, we assume that N measurements are collected, some of which correspond to some of the features and others to clutter. The proposed solution rests on defining a Markov chain $\{\theta_k\}$ such that each state corresponds to a unique combination of a motion model of the features, an obscuration/detection pattern, and an association of measurements to features.

To simultaneously estimate the states of all features of interest, we define an augmented state, x_k, as a concatenation (in some predefined order) of the individual feature (column) states. Likewise, the augmented measurement is obtained by concatenating all the measurements. The augmented measurement noise is obtained in a similar manner. It remains to describe the structure of the matrices $A(\theta_k)$, $C(\theta_k)$, $H(\theta_k)$, and $G(\theta_k)$ of the augmented system.

Since all features evolve identically, the augmented dynamics matrix is a block-diagonal matrix, where each block corresponds to a different feature. Since there are several motion models, $A(\theta_k)$ takes the following values

$$A(\theta_k) \in \left\{\mathrm{diag}(A^1, \dots, A^1), \dots, \mathrm{diag}(A^\ell, \dots, A^\ell)\right\},$$

where the number of blocks in $\mathrm{diag}(A^i, \dots, A^i)$, $i = 1, \dots, \ell$ is the number of features, L. Since all features share the same process noise, $C(\theta_k)$ takes the following values

$$C(\theta_k) \in \left\{ \begin{pmatrix} C^1 \\ \vdots \\ C^1 \end{pmatrix}, \dots, \begin{pmatrix} C^\ell \\ \vdots \\ C^\ell \end{pmatrix} \right\}.$$

We proceed with describing the structure and feasible values for the matrices of the measurement equation, $H(\theta_k)$, and $G(\theta_k)$. Recall that the augmented measurement noise is a concatenation of the measurement noises of the individual measurements, which may be true detections or clutter. Since the measurement noises of different measurements are independent, the matrix $G(\theta_k)$ is a block diagonal matrix with elements along its main diagonal being C (defined in (2)) and G_{cl} (defined at the end of Section II). The indices of the entries with C and G_{cl} correspond, respectively, to the locations of true and clutter measurements in the measurement vector. For example, the realization

$$\mathrm{diag}(G, \dots, G)$$

corresponds to the case where all features are detected; for

$$\mathrm{diag}(C, G_{\mathrm{cl}}, \dots, G_{\mathrm{cl}})$$

only the first measurement is a feature detection.

Recalling that the augmented state vector is a concatenation of the state of the L features, the structure of the matrix $H(\theta_k)$ follows from the following observations. The matrix comprises $N \times L$ blocks. Each of the blocks has the dimensions of the matrix H defined in (2). Every (block) row corresponds to either true or clutter measurement. In the latter case the row comprises only zero blocks. Rows corresponding to true detections have a single nonzero block which is H. For example, for the case with three features, all of which are detected and without clutter, we have the following options for $H(\theta_k)$

$$\begin{pmatrix} H & 0 & 0 \\ 0 & H & 0 \\ 0 & 0 & H \end{pmatrix}, \begin{pmatrix} 0 & H & 0 \\ H & 0 & 0 \\ 0 & 0 & H \end{pmatrix}, \begin{pmatrix} H & 0 & 0 \\ 0 & 0 & H \\ 0 & H & 0 \end{pmatrix}$$
$$\begin{pmatrix} 0 & 0 & H \\ H & 0 & 0 \\ 0 & H & 0 \end{pmatrix}, \begin{pmatrix} 0 & H & 0 \\ 0 & 0 & H \\ H & 0 & 0 \end{pmatrix}, \begin{pmatrix} 0 & 0 & H \\ 0 & H & 0 \\ H & 0 & 0 \end{pmatrix}.$$

These correspond to all possible associations of the three measurements to the three features.

Each state of the mode sequence $\{\theta_k\}$ corresponds to a feasible combination of the values of the above matrices. For example, in the second variant of the feature detection process (Section II), the values of $A(\theta_k)$ for which some of the features are obscured are not compatible with the values of $H(\theta_k)$ for which all the features are detected. The transition probabilities between different mode values are defined by the known transitions between different maneuvering regimes and the reasonable assumption that any association of measurements to features or clutter is equiprobable. To demonstrate the latter statement, assume that there are $L = 2$ features, two measurements and a single motion model (e.g., the target does not maneuver). Then the states of the resulting Markov chain $\{\theta_k\}$ are specified by the feasible values of $H(\theta_k)$ as follows

$$\begin{array}{ccccccc} 1 & 2 & 3 & 4 & 5 & 6 & 7 \\ \left(\begin{smallmatrix} H & 0 \\ 0 & H \end{smallmatrix}\right) & \left(\begin{smallmatrix} 0 & H \\ H & 0 \end{smallmatrix}\right) & \left(\begin{smallmatrix} H & 0 \\ 0 & 0 \end{smallmatrix}\right) & \left(\begin{smallmatrix} 0 & H \\ 0 & 0 \end{smallmatrix}\right) & \left(\begin{smallmatrix} 0 & 0 \\ H & 0 \end{smallmatrix}\right) & \left(\begin{smallmatrix} 0 & 0 \\ 0 & H \end{smallmatrix}\right) & \left(\begin{smallmatrix} 0 & 0 \\ 0 & 0 \end{smallmatrix}\right) \end{array}$$

and the corresponding TPM has the structure shown in Eq. (10) where $\mathbf{1}_{7\times 1}$ is a 7×1 vector comprising all ones and the symbol $\otimes$ stands for the Kronecker matrix product.

We note in passing that the described method makes full enumeration of all possible association events, and thus may be inefficient when many features are chosen, or at high clutter rates. However, since the focus of the paper is the unified modeling, we do not directly address herein this computational drawback. In addition, such a drawback is typical of multitarget data association problems. For example, in the Joint Probabilistic Data Association (JPDA) method [12], direct computation of the association probabilities is related to computing the permanent of a binary matrix [13] which is known to be a #P-complete [14] rendering JPDA an NP-hard problem. To overcome this obstacle additional approximations must be utilized. These are mainly based on gating, hypotheses pruning and merging, as discussed in, e.g., [15]. Applying similar approximations within the proposed framework of a unified modeling of data association problems may be an interesting research question by itself and is needed to allow computational feasibility of the approach.

V. NUMERICAL EXAMPLE

To demonstrate the proposed approach, we consider an aircraft with 3 feature points to be tracked. The chosen feature points are the center of the fuselage (marked as feature “1”) and the left and right wing-tips (marked as features “2” and “3”, respectively). The distance between the wing-tips (features ”2” and ”3”) and feature ”1” is 3 meters. The target flies at straight and level flight for 20 seconds and then performs an S-maneuver by making a 30 seconds long left coordinated turn, followed by a 40 seconds long straight and level leg and a 30 seconds long right coordinated turn. The final 20 seconds of the trajectory are another straight and level leg. The left and right coordinated turns are accomplished by performing an appropriate roll maneuver during which one of the wing-tips becomes obscured from the sensor’s field of view. For the present example, we consider the second variant of the feature detection process described in Section II. Namely, the features get obscured (and thus undetected) for some maneuvers. In our example, features “2” and “3” go undetected when performing left and right turns, respectively.

In addition, at each sampling time, each of the visible features is detected with probability $P_d = 0.95$ and goes undetected with probability $1 - P_d$.

For simplicity of the exposition, we assume that in the detection process some raw sensor data (which may be radar signals or grey levels of a digital camera) are thresholded and the three strongest returns are declared as measurements to be processed by the algorithm at the current time step. This is due to the possibility of obtaining clutter returns which occur due to, e.g., thermal noise in the sensor. Hence, whenever a feature is undetected (or obscured) a clutter measurement is obtained. This measurement is assumed to have uniform spatial distribution and does not carry valuable information about the features of interest.

The trajectory and a typical realization of the measurements is presented on the left of Fig. 1.

The IMM algorithm was designed using standard motion models – a nearly constant velocity (CV) model in two dimensions for the nonmaneuvering sections, and two coordinated turns (CT) models with known turn rates for the maneuvering sections (see [16]). The CV model is characterized by the following matrices for each feature in each of the two cartesian directions

$$A_{\mathrm{CV,1D}} = \begin{pmatrix} 1 & T \\ 0 & 1 \end{pmatrix}, \quad C_{\mathrm{CV,1D}} = \begin{pmatrix} T^2/2 \\ T \end{pmatrix},$$

where T is the sampling interval.

The CT model, which is inherently defined in two dimensions, is characterized by the following dynamics matrix

$$A_{\mathrm{CT}} = \begin{pmatrix} 1 & \sin(\omega T)/\omega & 0 & -(1-\cos(\omega T))/\omega \\ 0 & \cos(\omega T) & 0 & -\sin(\omega T) \\ 0 & (1-\cos(\omega T))/\omega & 1 & \sin(\omega T)/\omega \\ 0 & \sin(\omega T) & 0 & \cos(\omega T) \end{pmatrix},$$

where ω is the known turn rate. The matrix C_{CT} is constructed similarly to the CV model:

$$C_{\mathrm{CT}} = \begin{pmatrix} T^2/2 & 0 \\ T & 0 \\ 0 & T^2/2 \\ 0 & T \end{pmatrix}.$$

The chosen process noise levels were 0.3 m/s^2 for the nonmaneuvering regime and 0.6 m/s^2 for the maneuvering ones. The transitions between motion regimes were described by a Markov chain with transition probabilities

$$\begin{pmatrix} 0.8 & 0.1 & 0.1 \\ 0.3 & 0.7 & 0 \\ 0.3 & 0 & 0.7 \end{pmatrix}$$

and the initial distribution was taken to be uniform over those states that correspond to the CV motion model.

The standard deviation of the measurement noises was 0.5 meters and the clutter was taken to be uniform with standard deviation of 35 meters.

The resulting estimates, obtained by a single IMM, are presented on the right of Fig. 1. It is readily seen that the algorithm is capable of maintaining tracks of reasonable quality for all the features of interest.

For better visualization, we present in Fig. 2 the trajectories along with the corresponding estimates and the raw measurements, for two selected time intervals in each of the two directions separately.

For further illustration we present in Fig. 3 the probabilities of the different motion regimes of the target as computed by

$$\mathbf{1}_{7\times 1} \otimes \left(\tfrac{1}{2}P_d^2 \quad \tfrac{1}{2}P_d^2 \quad \tfrac{1}{4}P_d(1-P_d) \quad \tfrac{1}{4}P_d(1-P_d) \quad \tfrac{1}{4}P_d(1-P_d) \quad \tfrac{1}{4}P_d(1-P_d) \quad (1-P_d)^2\right) \tag{10}$$

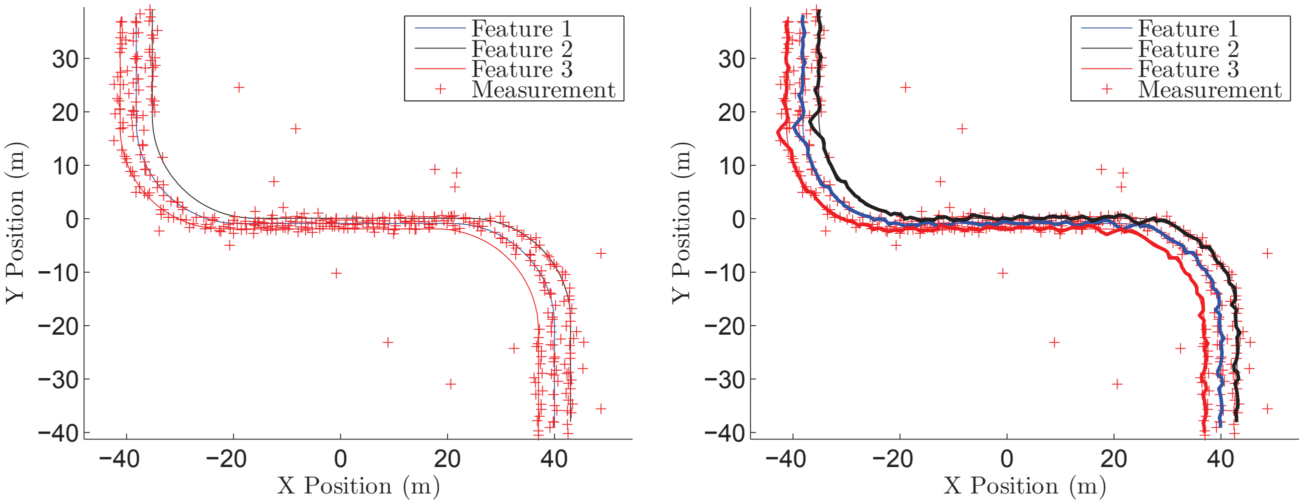

Fig. 1: The trajectories of the three features and sensor measurements (left). During maneuvering portions of the trajectory one of the features is obscured. The thick lines on the right are the resulting estimates obtained by a single IMM.

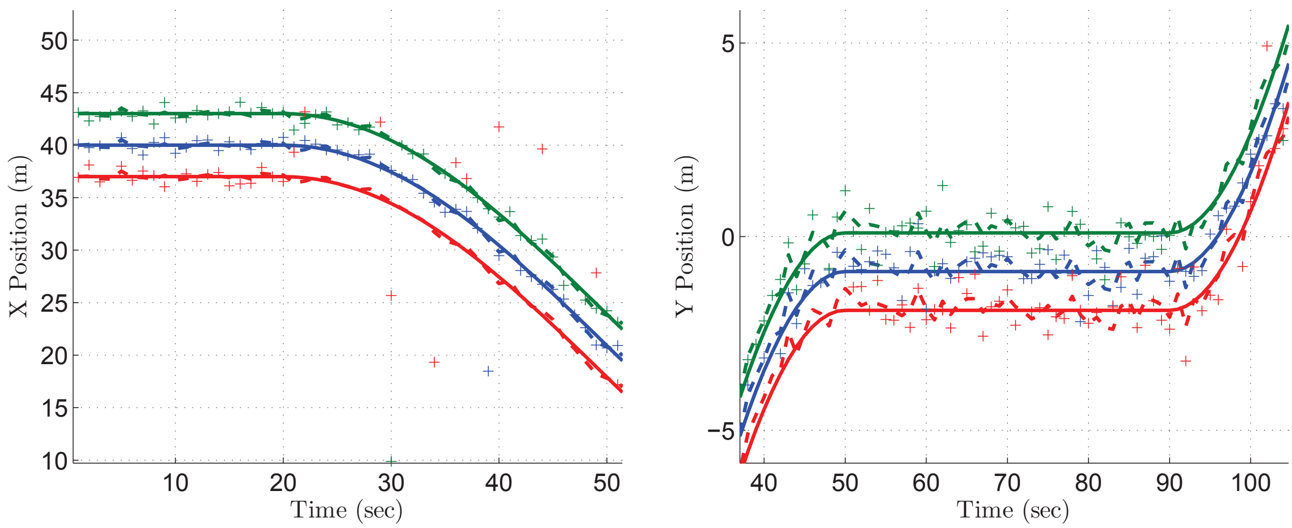

Fig. 2: The trajectories (solid lines) and the corresponding estimates (dashed lines) in the X direction (left) and in the Y direction (right) during selected time intervals.

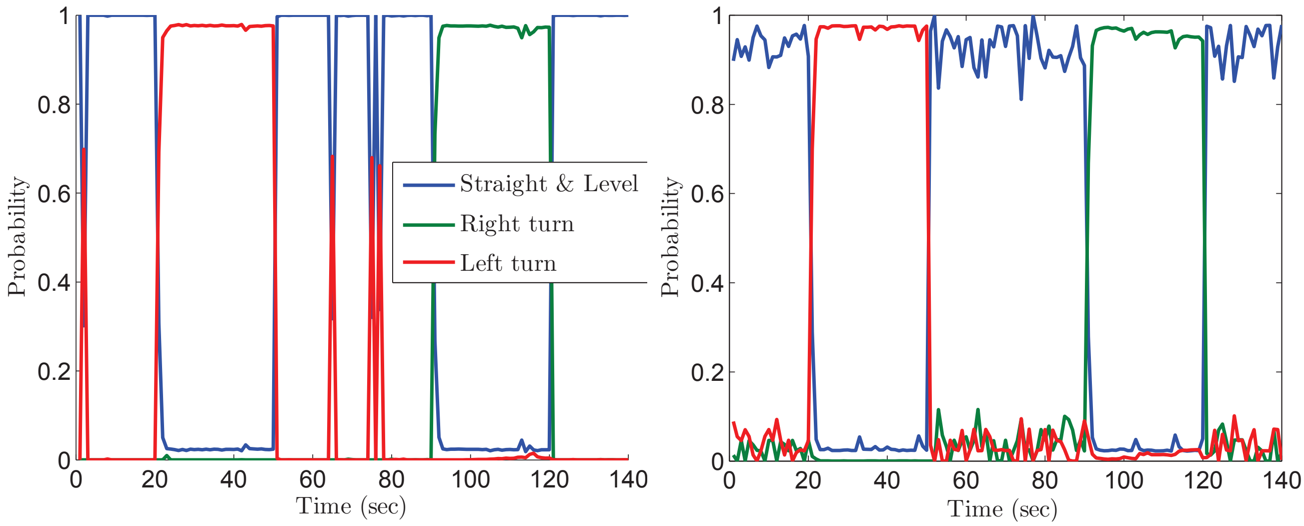

Fig. 3: The IMM probabilities of the different motion regimes. Single run (left), averaged over 20 Monte Carlo runs (right).

the algorithm. These are computed by summing the posterior probabilities of all modes corresponding to the same motion model. It is readily seen that all motion regimes are successfully identified.

We next perform a short sensitivity analysis in which the algorithm is tested in a series of experiments. For simplicity, we consider the maximal position error (in either direction) among all features as the performance measure.

TABLE I: Maximal Position Error vs. Measurement Noise

G (m)	0.5	1	1.5	2
Max. Error (m)	1.09	2.04	2.57	2.97

In Table I we summarize the maximal error versus measurement noise standard deviation. Recalling that the physical separation between adjacent features is 3 meter, we conclude that the algorithm is not capable of dealing with measurement noises higher than $G = 1.5(m)$ which introduce practical impossible ambiguity with respect to the locations of the features.

In Table II we test the performance for several detection probabilities. It is readily seen that the degradation in performance is graceful with error of 1.5 meters maintained at 80% detection rate.

TABLE II: Maximal Position Error vs. Detection Probability

P_d	0.95	0.9	0.85	0.8
Max. Error (m)	1.09	1.15	1.42	1.59

VI. CONCLUSION

We considered the problem of tracking an extended object and showed how it may be formulated within the framework of a single dynamical system with random coefficients. Consequently, the states of the features of interest may be estimated, in a straightforward manner, using a standard IMM algorithm. We demonstrated the utility of the method on a simple problem of tracking the features of a maneuvering target. It should be noted that this problem can serve as an example of the general approach originally presented by the authors in [9]. A simple example of the methodology may be found in [8], and for a more sophisticated one the reader is referred to [10]. Finally, focusing on the unified modeling, we did not address the inherent computational obstacles typical of multitarget data association problems. These need to be addressed by carefully incorporating additional approximations before the approach may be applied to real-life problems.

ACKNOWLEDGMENT

This research was supported by the Israeli Science Foundation under grant No. 1608/11.

REFERENCES

[1] O. E. Drummond, S. S. Blackman, and G. C. Petrisor, "Tracking clusters and extended objects with multiple sensors," in *Proceedings of Signal and Data Processing of Small Targets*, vol. 1305, pp. 362–375, 1990.

[2] J. Dezert, "Tracking maneuvering and bending extended target in cluttered environment," in *Proceedings of Signal and Data Processing of Small Targets*, vol. 3373, pp. 283–294, 1998.

[3] J. W. Koch, "Bayesian approach to extended object and cluster tracking using random matrices," *IEEE Trans. Aerosp. Electron. Syst.*, vol. 44, no. 3, pp. 1042–1059, 2008.

[4] N. Ikoma and S. Godsill, "Extended object tracking with unknown association, missing observations, and clutter using particle filters," in *2003 IEEE Workshop on Statistical Signal Processing*, pp. 502–505, IEEE, 2003.

[5] J. Vermaak, N. Ikoma, and S. J. Godsill, "Sequential Monte Carlo framework for extended object tracking," in *IEE Proceedings-Radar, Sonar and Navigation*, vol. 152, pp. 353–363, IET, 2005.

[6] M. Baum and U. D. Hanebeck, "Extended object tracking with random hypersurface models," *arXiv preprint arXiv:1304.5084*, 2013.

[7] H. Blom and Y. Bar-Shalom, "The interacting multiple model algorithm for systems with Markovian switching coefficients," *IEEE Trans. Autom. Control*, vol. 33, no. 8, pp. 780–783, 1988.

[8] D. Sigalov, T. Michaeli, and Y. Oshman, "LMMSE filtering in feedback systems with white random modes: Application to tracking in clutter," *IEEE Trans. Autom. Control*. to appear.

[9] D. Sigalov, T. Michaeli, and Y. Oshman, "A unified approach to state estimation problems under data and model uncertainties," in *Proc. Fusion 2012, 15th Int. Conf. on Information Fusion*, IEEE, 2012.

[10] D. Sigalov, T. Michaeli, and Y. Oshman, "Tracking a splitting target in clutter using the IMM methodology," in *Proc. 27th Convention of Electrical and Electronis Engineers in Israel.*, IEEE, 2012.

[11] Y. Bar-Shalom, X. Li, and T. Kirubarajan, *Estimation with Applications to Tracking and Navigation*. New York : Wiley, 2001.

[12] T. Fortmann, Y. Bar-Shalom, and M. Scheffe, "Sonar tracking of multiple targets using joint probabilistic data association," *IEEE J. Ocean. Eng.*, vol. 8, no. 3, pp. 173–184, 1983.

[13] J. Collins and J. Uhlmann, "Efficient gating in data association with multivariate distributed states," *IEEE Trans. Aerosp. Electron. Syst.*, vol. 28, pp. 909–916, July 1992.

[14] L. G. Valiant, "The complexity of computing the permanent," *Theoretical computer science*, vol. 8, no. 2, pp. 189–201, 1979.

[15] Y. Bar-Shalom and X. Li, *Multitarget-Multisensor Tracking: Principles and Techniques*. Storrs, CT: YBS Publishing, 1995.

[16] X. Li and V. Jilkov, "Survey of maneuvering target tracking. Part I: Dynamic models," *IEEE Trans. Aerosp. Electron. Syst.*, vol. 39, no. 4, p. 1333, 2003.